Journal of Radioanalytical and Nuclear Chemistry (2025) 334:5149–5154
https://doi.org/10.1007/s10967-025-10178-z

Cross-section measurements of the ^{93}Nb(p,n)^{93m}Mo reaction up to 17 MeV

Andreas Dragoun[1,2] · Ingo Spahn[2] · Mazhar Hussain[2,3] · Erik Strub[1] · Bernd Neumaier[1,2,4] · Johannes Ermert[1,2]

Received: 10 April 2025 / Accepted: 9 May 2025 / Published online: 31 May 2025

Abstract
The nuclear reaction cross-sections of the ^{93}Nb(p,n)^{93m}Mo process were measured in three experiments up to 17 MeV proton energy by using the stacked target foil technique. The target stacks were irradiated at the cyclotron JSW BC 1710 at the Forschungszentrum Jülich, INM-5. The ^{nat}Cu(p,x)$^{62/63}$Zn reactions were used as monitor reactions to determine the proton particle flux and the incident proton energy. The experimental results were compared with literature data and with theoretical nuclear model calculations based on the TALYS-1.96 code and the data from TENDL-2023. Furthermore, it could be shown that the ^{93}Nb(p,n)^{93m}Mo reaction delivers sufficient amounts of activity for the later application of ^{93m}Mo as a tracer to optimize the radiochemical separation of low specific activity ^{99}Mo and ^{99m}Tc.

Keywords Cross-section · Excitation function · Cyclotron irradiation · Targetry · Molybdenum-93m

Introduction

Nuclear data are of significant importance across a wide range of research areas and applications, particularly in the context of evaluating the validity of nuclear models and the production of medical radionuclides and other tracer nuclides. ^{99}Mo, the parent of the world´s most widely used medical radionuclide, ^{99m}Tc, is almost exclusively produced in nuclear research reactors by the fission of highly enriched ^{235}U, which poses a threat of proliferation. In addition, there have been repeated supply shortages of ^{99}Mo in the past due to maintenance work on the ageing nuclear reactors and unexpected reactor shutdowns. To address these problems, among others, the joint project *^{99}MoBest* was initiated by the German Federal Ministry of Research, Technology and Space (BMFTR) to develop alternative production routes for ^{99}Mo using accelerator-based technologies to avoid the use of fissile material. However, these alternative production methods will produce ^{99}Mo with low specific activity, making it necessary to adapt the established ^{99}Mo/^{99m}Tc generator system for the use of ^{99}Mo with low specific activity. Therefore, ^{93m}Mo was selected as a tracer to optimize the radiochemical separation of ^{99}Mo and ^{99m}Tc. The radionuclide ^{93}Mo has a ground state ^{93g}Mo (half-life of 4.0×10^3 y; spin 5/2+), and a metastable isomer ^{93m}Mo (half-life of 6.85 h; spin 21/2+). The excited state decays almost exclusively (99.8832%) via isomeric transition to the ground state and by beta plus decay (0.1169%) to ^{93}Nb [1]. During the decay, three high-intensity gamma lines (263.1, 684.7 and 1477.2 keV) are emitted, which are suitable for identification and activity determination. To optimize the cyclotron production of ^{93m}Mo, it is essential to know the exact excitation function. Furthermore, at higher energies, the ^{93}Nb(p,4n)^{90}Mo reaction can be used as a proton beam monitor [2]. The excitation function of the ^{93}Nb(p,n)^{93m}Mo nuclear reaction has been reported in the literature [3–9]. However, these data sets show inconsistencies, which require a critical review.

✉ Bernd Neumaier
b.neumaier@fz-juelich.de

1 Division of Nuclear Chemistry, Department of Chemistry and Biochemistry, Faculty of Mathematics and Natural Sciences, University of Cologne, 50674 Cologne, Germany

2 Institute of Neuroscience and Medicine – Nuclear Chemistry (INM-5), Forschungszentrum Jülich GmbH, 52525 Jülich, Germany

3 Department of Physics, Government College University Lahore (GCUL), Lahore 5400, Pakistan

4 Institute of Radiochemistry and Experimental Molecular Imaging, Faculty of Medicine and University Hospital Cologne, University of Cologne, 50937 Cologne, Germany

In this work, we aimed to comprehensively evaluate the excitation function up to 17 MeV, using experimental data and nuclear model calculations performed with the TALYS-1.96 code. The $^{nat}Cu(p,x)^{62/63}Zn$ monitor reactions were used to determine the proton energy and proton flux. The nuclear reaction cross-sections were calculated by using the activation equation.

Experimental

Target preparation

For the activation experiments at the cyclotron, the stacked-foil technique [10] was used. Each target consisted of three distinct types of metal foils: niobium target foils (99.9% purity, 0.0075 mm thickness, Thermo Scientific), copper monitor foils (99.9% purity, 0.01 mm thickness, Goodfellow), and aluminum energy degrader foils (99.0% and 99.999% purity, 0.020 mm and 0.050 mm thickness, Goodfellow). The foils were cut into 13 mm diameter discs, weighed using an analytical balance (accuracy of 0.0001 g) and stacked in the screw-capped target holder, which was made of copper [11].

Irradiation and beam monitoring

The sequence of the foils in each target stack was based on calculations of the energy loss along the stack. These calculations were carried out using the Excel-based program *Stack*, written by Forschungszentrum Jülich based on the formalism of Bethe [12] and the tables of Williamson et al. [13]. A copper monitor foil was placed on the top of each stack to determine the incident proton energy and proton particle flux, employing the $^{nat}Cu(p,x)^{62/63}Zn$ monitor reactions as recommended by the IAEA [14] and Hermanne et al. [15], and the ratio of ^{62}Zn and ^{63}Zn as described by Piel et al. [16]. The proton irradiations were conducted at the JSW Baby Cyclotron BC 1710 at the INM-5. The target stacks were irradiated for 30 min with an incident proton beam energy of 17 MeV and a bream current of 1 µA.

Measurement of radioactivity

Following the irradiations, the target stacks were disassembled and the activity of the niobium and copper foils was determined by gamma-ray spectrometry using a high-resolution HPGe gamma-ray detector (Ortec, GEM-20190). The measured count rates were converted into decay rates, considering the corresponding γ-ray emission probability and the efficiency of the detector. The efficiency of the HPGe γ-ray detector was determined with standard gamma-ray point sources (^{241}Am, ^{133}Ba, ^{57}Co, ^{60}Co, ^{137}Cs, ^{152}Eu, and ^{54}Mn from Eckert & Ziegler). The detector efficiency calibration was performed for different distances between the sample and the detector. For each measurement, a sufficiently large distance was chosen to minimize the dead time (< 10%) and reduce the coincident summing effect. To ensure adequate statistical uncertainties of ≋1% the counting times were adjusted accordingly. The decay data used for identifying and measuring the activity of the reaction products were obtained from the Live Chart of Nuclides [1] of the IAEA and are given in Table 1. A typical γ-ray spectrum of a niobium foil irradiated with 12.8 MeV protons is shown in Fig. 1. The measured γ-ray spectra were analyzed using GammaVision software (version 8.10.02, Advanced Measurement Technology, Inc.), which can determine the energy and number of counts of the photopeaks.

Calculation of cross-sections and uncertainties

The cross-section values were calculated using the well-known activation equation. The total uncertainty in each cross-section value was obtained by error propagation, considering the following uncertainties: mass of the metal foils (1%), peak area (statistical uncertainty; 0.8 to 3.4%), peak efficiency (uncertainty of the fitted efficiency curve; 1.3 to 1.6%), decay data (1%), and calculated proton flux (8%).

Table 1 Decay data [1] and production routes of the reaction products

Nuclide	Production route	Half-live	Decay mode (%)	Energy of gamma emission (keV)	Intensity of gamma emission (%)
^{93m}Mo	$^{93}Nb(p,n)$	6.85 h	IT (99.88); EC + β^+ (0.12)	263.05	57.4
				684.69	99.9
				1477.14	99.1
^{62}Zn	$^{nat}Cu(p,x)$	9.193 h	EC + β^+ (100)	548.35	15.3
				596.56	26.0
^{63}Zn	$^{nat}Cu(p,x)$	38.47 min	EC + β^+ (100)	669.64	8.2
				962.06	6.5

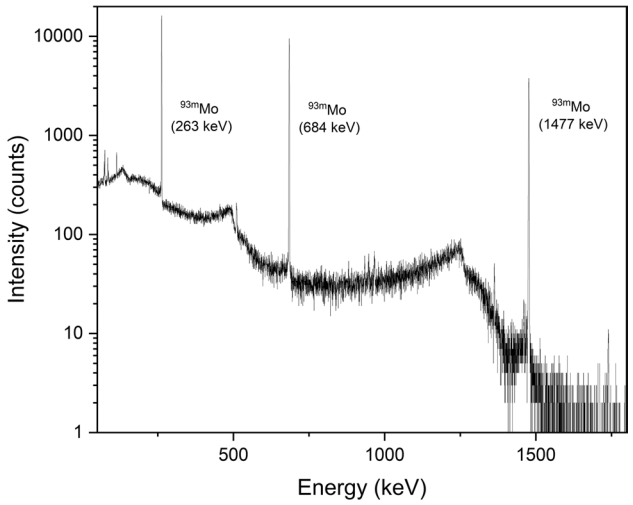

Fig. 1 Typical γ-ray spectrum of a niobium foil irradiated with 12.8 MeV protons measured five hours after the end of bombardment, showing the three most intense gamma-ray signals of ^{93m}Mo. By-products could not be observed

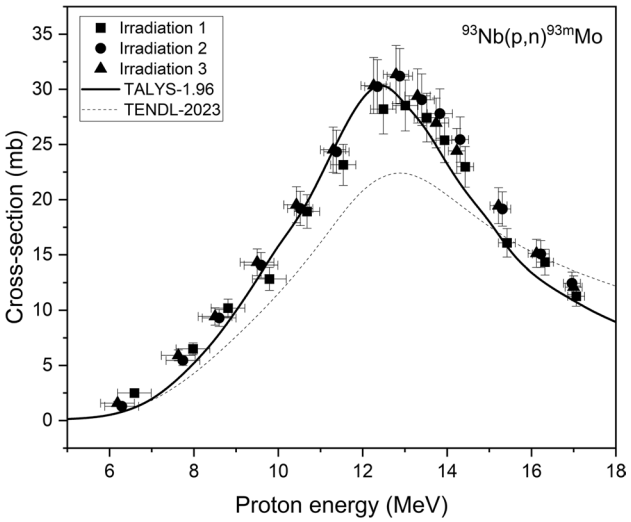

Fig. 2 Experimental cross-sections of the ^{93}Nb(p,n).^{93m}Mo reaction of the present work compared with theoretical nuclear model calculations by TALYS-1.96 and the TENDL- 2023 data [21]

The total uncertainty in each measured cross-section value ranged from 8 to 8.7%.

Theoretical calculations

Different codes are available for the simulation of nuclear cross-sections [15]. The TALYS code has been developed for the calculation of reaction cross-sections from 1 keV to 200 MeV [17, 18]. TALYS-1.96 is the most recent version for the validation and evaluation of experimental data. The input parameters are normally obtained from the RIPL-3 library of the IAEA [19]. The ECIS code, incorporated in TALYS implements the optical model and direct reaction mechanisms for the calculation. The continuum levels were calculated by the back-shifted Fermi gas model developed in the TALYS-1.96 code. The modified optical model potentials (OMPs) from the compilation of Koning and Delaroche were chosen for protons in all competing nuclear reactions [20]. The results obtained using general and modified parameters led to the generation of reaction cross-sections of the ^{93}Nb(p,n)-reaction for the formation of ^{93m}Mo. The calculated results are shown in Fig. 2 together with TENDL-2023 data [21] for comparison.

Results and discussion

Cross-sections

The experimental cross-sections and their associated uncertainties derived from the three irradiations presented in this study are listed in Table 2. These are illustrated alongside theoretical calculations obtained from TALYS and data from TENDL-2023 [21] in Fig. 2.

As illustrated in Fig. 2, cross-section values of all three irradiations are consistent within the uncertainties. The cross-sections of irradiation 1 seem to be somewhat shifted to lower values yet remain within the range of measurement uncertainties. The experimental cross-sections of the present study and recent literature data from Avila-Rodriguez et al. [3], Ditrói et al. [4], Kim et al. [5], Lawriniang et al. [6], Parashari et al. [7], Rizvi et al. [8] and Levkovskij [9] are compared in Fig. 3. It should be noted that some older literature values, including those from Blaser et al. [22], Forsthoff et al. [23], and James [24], were not considered in this study and the focus was on comparison with more recent literature. The measured cross-sections follow the general trend of the literature curves and are in good agreement with the data reported by Avila-Rodriguez et al. and Ditrói et al. In contrast, the data of Ditrói et al. are somewhat scattered. The data presented by Lawriniang et al. and Kim et al. tend to underestimate the cross-section in certain regions of the excitation function. In particular, the three measured values in the range of the maximum of the excitation function of Kim et al. are significantly lower than our data and the other literature values. Furthermore, the cross-sections from Rizvi et al. are shifted to higher values in the lower energy region. The cross-sections from Levkovskij [9] are generally shifted to lower energies compared to the other literature values and our experimental data. The theoretical values derived from the TALYS calculations are in accordance with the experimental cross-sections of our study. However, above 13 MeV,

Table 2 Experimental cross-sections of ^{93}Nb(p,n)^{93m}Mo reaction

Irradiation 1		Irradiation 2		Irradiation 3	
Proton energy (MeV)	Cross- section (mb)	Proton energy (MeV)	Cross-section (mb)	Proton energy (MeV)	Cross- section (mb)
17.1 ± 0.2	11.3 ± 1.0	17.0 ± 0.2	12.4 ± 1.0	17.0 ± 0.2	12.1 ± 1.0
16.3 ± 0.2	14.3 ± 1.2	16.2 ± 0.2	15.1 ± 1.2	16.1 ± 0.2	15.1 ± 1.3
15.4 ± 0.2	16.1 ± 1.3	15.3 ± 0.2	19.2 ± 1.6	15.2 ± 0.2	19.4 ± 1.6
14.4 ± 0.2	23.0 ± 1.8	14.3 ± 0.2	25.4 ± 2.1	14.2 ± 0.2	24.4 ± 2.0
13.9 ± 0.3	25.4 ± 2.0	13.8 ± 0.3	27.8 ± 2.2	13.7 ± 0.3	27.0 ± 2.3
13.5 ± 0.3	27.4 ± 2.2	13.4 ± 0.3	29.1 ± 2.3	13.3 ± 0.3	29.4 ± 2.5
13.0 ± 0.3	28.5 ± 2.3	12.9 ± 0.3	31.2 ± 2.5	12.8 ± 0.3	31.4 ± 2.6
12.5 ± 0.3	28.2 ± 2.3	12.4 ± 0.3	30.2 ± 2.4	12.3 ± 0.3	30.4 ± 2.5
11.5 ± 0.3	23.2 ± 1.9	11.4 ± 0.3	24.3 ± 2.0	11.3 ± 0.3	24.5 ± 2.1
10.7 ± 0.3	18.9 ± 1.5	10.5 ± 0.3	19.2 ± 1.6	10.4 ± 0.3	19.5 ± 1.6
9.8 ± 0.4	12.8 ± 1.0	9.6 ± 0.4	14.1 ± 1.1	9.5 ± 0.4	14.3 ± 1.2
8.8 ± 0.4	10.2 ± 0.8	8.6 ± 0.4	9.3 ± 0.8	8.5 ± 0.4	9.4 ± 0.8
8.0 ± 0.4	6.5 ± 0.5	7.7 ± 0.4	5.5 ± 0.5	7.6 ± 0.4	5.9 ± 0.5
6.6 ± 0.4	2.5 ± 0.2	6.3 ± 0.4	1.3 ± 0.1	6.2 ± 0.4	1.6 ± 0.1

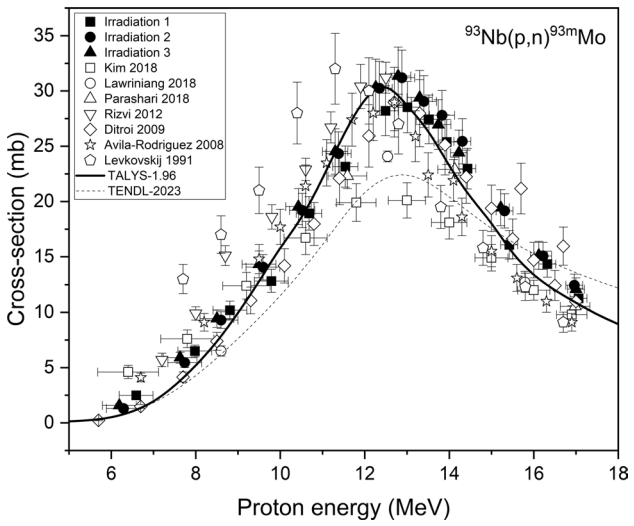

Fig. 3 Comparison of experimental cross-sections with literature data of the ^{93}Nb(p,n).^{93m}Mo reaction and theoretical calculation obtained from TALYS-1.96 and TENDL-2023 [21]

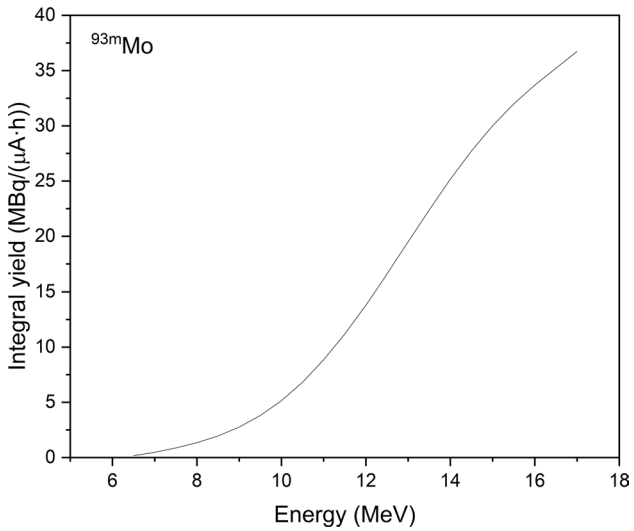

Fig. 4 Integral yields for the production of ^{93m}Mo

a slight shift towards higher energies is observed for the data presented in this work. The theoretical TALYS calculations show better agreement with our experimental data values than the TENDL-2023 data. The crosssections from TENDL are much lower compared to most of the literature values, except the data from Kim et al. Compared to many other (p,n)-reactions in this mass region, the cross-section value for the ^{93}Nb(p,n)^{93m}Mo reaction is rather small [25]. There are possibly two reasons: (1) cross-sections for metastable states are generally lower than the total (p,n) cross-section; (2) the very high-spin isomer (spin 21/2 +) is not favorably populated at low projectile energies used in this work [26, 27].

Integral yields

The integral yields for the production of ^{93m}Mo were calculated based on the measured cross-sections corresponding to an irradiation period of 1 h and a beam current of 1 μA and are given in Fig. 4. By irradiating ^{93}Nb for one hour with a beam current of 1 μA in the energy region around the maximum of the excitation function (between 11 and 13 MeV), a ^{93m}Mo activity of 12.7 MBq can be obtained. This amount of

activity is sufficient for the planned use of ^{93m}Mo as a tracer to optimize the radiochemical separation of low specific activity ^{99}Mo and ^{99m}Tc. In the literature, some single values are known for certain energies, e.g. [28–31], but no complete yield curve. Sadeghi et al. [28] report a yield of 19 MBq/μA•h at an energy of 12.5 MeV, which is close to our value reported in Fig. 4. The other yield data from Abe et al. [29] (269 μCi/μA•h, respectively 10 MBq/μA•h; 15.5 MeV), Isshiki et al. [30] (6400 μCi/μA•h, respectively 237 MBq/μA•h; 10.4 MeV) and Nickles [31] (1.7 mCi/μA, respectively 63 MBq/μA; 11 MeV) show large deviations from our experimental data.

Conclusions

The excitation function of the ^{93}Nb(p,n)^{93m}Mo reaction was measured three times up to proton energies of 17 MeV using the stacked foil technique with an overall uncertainty of 8 to 8.7%. The experimental cross-sections were compared with literature data and theoretical values obtained from calculations conducted with TALYS-1.96. It was observed that the excitation functions from the present work were in good agreement with the theoretical TALYS code calculations and with most of the literature values, except for the TENDL-2023 data. It was also shown that the ^{93}Nb(p,n)^{93m}Mo provides sufficient activity for the future application of ^{93m}Mo as a tracer in radiochemical separations of low activity ^{99}Mo and ^{99m}Tc.

Acknowledgements The authors would like to express their gratitude to Stefan Spellerberg, Marina Birr and Ingo Montag for conducting the cyclotron irradiations at the INM-5. Furthermore, the authors would like to acknowledge Syed M. Qaim for his contributions to the project through discussions and guidance.

Author contributions A. Dragoun: Conceptualization, investigation, data curation, visualization, writing – original draft, writing – review & editing. I. Spahn: Investigation, validation. M. Hussain: Theoretical calculations. E. Strub: Validation. B. Neumaier: Supervision, writing – review & editing. J. Ermert: Supervision, conceptualization.

Funding Open Access funding enabled and organized by Projekt DEAL. This work is part of the*^{99}MoBest collaborationand received funding by the German Federal Ministry of Research, Technology and Space (BMFTR) under grant No. 02NUK080A.*

Declarations

Conflict of interests The authors declare they have no known competing financial interests that could have appeared to influence the work reported in this paper. The author B. Neumaier is Associate Editor of the *Journal of Radioanalytical and Nuclear Chemistry.*

References

1. IAEA Live Chart of Nuclides, https://www-nds.iaea.org/relnsd/vcharthtml/VChartHTML.htnml
2. Tárkanyi F, Hermanne A, Ignatyuk AV, Ditrói F, Takács S, Capote-Noy R (2024) Extension of evaluated cross section database for charged particle monitor reactions. J Radioanal Nucl Chem 333:4243–4331
3. Avila-Rodriguez MA, Wilson JS, Schueller MJ, McQuarrie SA (2008) Measurement of the activation cross section for the (p,xn) reactions in niobium with potential applications as monitor reactions. Nucl Instrum Methods Phys Res B 266:3353–3358
4. Ditrói F, Hermanne A, Corniani E, Takács S, Tárkányi F, Csikai J, Shubin YuN (2009) Investigation of proton induced reactions on niobium at low and medium energies. Nucl Instrum and Methods in Phys Res B 267:3364–3374
5. Kim K, Kim G, Shahid M, Zaman M, Yang S-C, Uddin MdS, Naik H (2018) Excitation functions of ^{93}Nb(p,x) reactions from threshold to 42.4 MeV. J Radioanal Nucl Chem 317:1021–1031
6. Lawriniang B, Ghosh R, Badwar S, Vansola V, Santhi Sheela Y, Suryanarayana SV, Naik H, Naik YP, Jyrwa B (2018) Measurement of cross-sections for the ^{93}Nb(p,n)^{93m}Mo and ^{93}Nb(p,pn)^{92m}Nb reactions up to ~20 MeV energy. Nucl Phys A 973:79–88
7. Parashari S, Mukherjee S, Nayak BK, Makwana R, Suryanarayana SV, Naik H, Sharma SC (2018) Excitation functions of the p + ^{93}Nb reaction in the energy range 10–22 MeV. Nucl Phys A 978:160–172
8. Rizvi IA, Kumar K, Ahmad T, Agarwal A, Chaubey AK (2012) Energy dependence of pre-equilibrium emission for the (p,xn) reactions in niobium. Indian J Phys 86(10):913–918
9. Levkovskij V N (1991) Levkovskij, Act. Cs. By Protons and Alphas, Moscow, USSR
10. Weinreich R, Schult O, Stöcklin G (1974) Production of ^{123}I via the ^{127}I(d,6n)^{123}Xe(β$^+$,EC)^{123}I process. Int J Appl Radiat Isot 25:535–543
11. Spellerberg S, Scholten B, Spahn I, Bolten W, Holzgreve M, Coenen HH, Qaim SM (2015) Target development for diversified irradiations at a medical cyclotron. Appl Radiat Isot 104:106–112
12. Bethe HA (1940) A continuum theory of the compound nucleus. Phys Rev 57:1125–1133
13. Williamson C F, Boujot J-P, Picard J (1966) Tables of range and stopping power of chemical elements for charged particles of energy 0.05 to 500 MeV. Rapport CEA-R 3042
14. IAEA Monitor Reactions, https://www-nds.oaea.org/medical/monitor_reactions.html
15. Hermanne A, Ignatyuk AV, Capote R, Carlson BV, Engle JW, Kellert MA, Kibédi T, Kim G, Kondev FG, Hussain M, Lebeda O, Luca A, Nagai Y, Naik H, Nicholas AL, Nortier FM, Suryanarayana SV, Takács S, Tárkányi FT, Verpelli M (2018) Reference cross sections for charged-particle monitor reactions. Nucl Data Sheets 148:338–382
16. Piel H, Qaim SM, Stöcklin G (1992) Excitation functions of (p,xn)-reactions on ^{nat}Ni and highly enriched ^{62}Ni: possibility of production of medically important radioisotope ^{62}Cu at a small cyclotron. Radiochim Acta 57:1–5
17. Koning AJ, Hilaire S, Goriely S (2023) TALYS: Modeling of nuclear reactions. Eur Phys J A 59:131

18. TENDL: TALYS global library, available at: TENDL-2021 nuclear data library (psi.ch)
19. Capote R, Herman M, Oblozinsky P, Young PG, Goriely S, Belgya T, Ignatyuk AV, Koning AJ, Hilaire S, Plujko VA, Avrigeanu M, Bersillon O, Chadwick MB, Fukahori T, Ge Z, Han Y, Kaila S, Kopecky J, Maslov VM, Reffo G, Sin M, Sh SE, Talou P (2009) RIPL – 3, reference input parameter library for calculation of nuclear reactions and nuclear data evaluations. Nucl Data Sheets 110:3107–3214
20. Koning AJ, Delaroche JP (2003) Local and global nucleon optical models from 1 keV to 200 MeV. Nucl Phys A 713:231–310
21. Koning AJ, Rochmann D, Sublet J, Dzysiuk N, Fleming M, van der Marck S (2019) Complete nuclear data library for innovative nuclear science and technology. Nucl Data Sheets 155:1–55
22. Blaser J-P, Boehm F, Marmier P, Peaslee D C (1951) Fonctions d´excitation de la reaction (p,n). Helv Phys Acta 24(1)
23. Forsthoff C, Gockermann R, Naumann R (1951) Formation and decay of Mo^{93m}. Phys Rev 90:1004–1005
24. James RA (1954) Excitation functions of proton-induced reactions of Nb^{93}. Phys Rev 93(2):288–290
25. Qaim SM, Mushtaq A (1988) Isomeric cross-section ratio for the formation of ^{73m,g}Se in various nuclear processes. Phys Rev C 38(2):645–650
26. Kastleiner S, Shubin YuN, Nortier FM, Van der Walt TN, Qaim SM (2004) Experimental studies and nuclear model calculations on (p,xn) and (p,pxn) reactions on ^{85}Rb from their thresholds up to 100 MeV. Radiochim Acta 92:449–454
27. Uddin MS, Sudár S, Basunia MS, Spahn I, Voyles AS, Hermanne A, Bernstein LA, Neumaier B, Qaim SM (2024) Cross sections for the formation of ^{84m,g}Rb, ^{83}Rb, and ^{82m}Rb in ^{86}Sr(d,x) reactions up to deuteron energies of 49 MeV: Competition between α-particle and multinucleon emission processes. Phys Rev C 110:064608
28. Sadeghi M, Enferadi M, Nadi H, Tenreiro C (2010) A novel method for the cyclotron production no-carrier-added ^{93m}Mo for nuclear medicine. J Radioanal Nucl Chem 286:141–144
29. Abe K, Iizuka A, Hasegawa A, Morozumi S (1984) Induced radioactivity of component materials by 16-MeV protons and 30-MeV alpha particles. J Nucl Mater 122&123:972–976
30. Isshiki M, Fukuda Y, Igaki K (1984) Proton activation analysis of trace impurities in purified cobalt. Radioanal Nucl Chem 82(1):135–142
31. Nickles RJ (1991) A shotgun approach to the chart of the nuclides. Radiotracer production with an 11 MeV proton cyclotron. Acta Radiol Suppl 376:69–71